Friction **10**(7): 1114–1126 (2022)
https://doi.org/10.1007/s40544-021-0554-9
ISSN 2223-7690
CN 10-1237/TH
RESEARCH ARTICLE

One-step method to enhance biotribological properties and biocompatibility of DLC coating by ion beam irradiation

Yuzhen LIU[1], Kelun ZHANG[2], Jae-Ho HAN[1], Youn-Hoo HWANG[1], Shusheng XU[3,*], Dae-Eun KIM[1,*]

[1] *Department of Mechanical Engineering, Yonsei University, Seoul 03722, Republic of Korea*

[2] *Department of Dermatology and Cutaneous Biology Research Institute, Yonsei University College of Medicine, Seoul 03722, Republic of Korea*

[3] *State Key Laboratory of Solid Lubrication, Lanzhou Institute of Chemical Physics, Chinese Academy of Sciences, Lanzhou 730000, China*

Received: 18 May 2021 / Revised: 25 August 2021 / Accepted: 14 September 2021

Abstract: A one-step method was developed to create a highly biocompatible micropatterned surface on a diamond-like carbon (DLC) through irradiation with a nitrogen ion beam and thus enhance the biocompatibility of osseointegrated surfaces and biotribological performance of articular surfaces. The biocompatibility and biotribological mechanisms were analyzed in terms of the structure and morphology of DLC. It was demonstrated that a layer enriched in sp^3 C–N bonds was formed on the surface of the DLC after nitrogen ion beam irradiation. Moreover, with an increase in the radiation dose, the content of sp^3 C–N on the DLC surface increased significantly, and the biocompatibility was positively correlated with it. The adhesion of the MC3T3 osteoblasts increased significantly from 32% to 86% under an irradiation dose of 8×10^{15} ions/cm^2. In contrast, the micropattern had a significant negative effect on the adhesion of the osteoblasts as it physically hindered cell expansion and extension. The micropattern with a depth of 37 nm exhibited good friction properties, and the coefficient of friction was reduced by 21% at relatively high speeds.

Keywords: ion beam irradiation; biocompatibility; diamond-like carbon (DLC); in-vivo; micropattern; biotribological performance

1 Introduction

Total joint replacement (TJR) is one of the most commonly performed medical interventions, and TJR implants need to reside in the body for a significant amount of time. This requires the implant to be biologically compatible with the host tissues and possess excellent biotribological properties to prolong its lifetime [1]. The failure of TJR is mainly due to infection and osteolysis caused by wear, loosening, stiffness, and instability [2, 3]. Infection problems arise from passive non-specific protein coatings, which may not optimally support adhesion of osteoblastic cells and enable bacterial adhesion [4, 5]. Osteolysis is an inflammatory reaction caused by wear particles and corrosion products that lead to bone resorption, which ultimately leads to loosening and failure of the artificial joint [6]. Therefore, to improve the longevity and stability of implants, various protective coatings have been proposed to enhance the surface biocompatibility and biotribological properties of implants [7, 8].

Diamond-like carbon (DLC) has emerged as a versatile and useful coating material owing to its distinct combination of chemical, mechanical, and thermal properties [9, 10]. DLC is harder than most ceramics, has a low coefficient of friction and high wear resistance, and thus, it can be used to improve the durability of precision parts, such as orthopedic implants [11]. Although substantial progress has been made in the development of DLC-based materials,

* Corresponding authors: Shusheng XU, E-mail: ssxu@licp.cas.cn; Dae-Eun KIM, E-mail: kimde@yonsei.ac.kr

their biocompatibility is still limited [12, 13]. The introduction of elements such as F, Cr, Si, Ti, or Ag into the DLC film can affect the adsorption ratio of different proteins that could affect cell adhesion and cell proliferation, thereby improving the biocompatibility of the coating [14–18]. However, fluoride and chromium compounds have potential toxicity risks, and the addition of silver may have cytotoxic effects on bone marrow cells and increase the risk of bone tissue resorption [9]. Moreover, the mechanical properties of DLC coatings are inevitably weakened, resulting in a compromise between mechanical and biological properties [7, 9]. These issues can be overcome by surface treatment through tailoring the coating surface to obtain desirable biological properties without altering the mechanical properties [19].

Various surface modification techniques have been utilized to optimize the biocompatibility of DLC coatings, such as plasma exposure [20], chemical attachment of specific molecules [21], and ion implantation [22]. Particularly, ion implantation through low-energy ion beam irradiation (ion energy ≤ 2,000 eV) introduces an appropriate number of ions into the surface layer of the coating to tailor the chemical properties without altering the overall mechanical strength because the penetration depth is generally less than 10 nm [22–24]. In addition, its line-of-sight nature allows the coating topography to be tailored for the fabrication of microscale patterns [25]. Generally, a micropattern can reduce friction and wear on the articular surface via the following three approaches: (i) lubricant reservoirs and wear debris trapping; (ii) micro-hydrodynamic effects; and (iii) reducing the nominal contact area [26].

In previous studies concerning DLC as a multifunctional coating used in orthopedic materials, the biotribological properties and biocompatibility of DLC showed limitations. In particular, DLC-based coatings demonstrated cell adhesion in the range of 20%–70% and insufficient lubrication performance in body fluid lubrication [7, 8, 22]. In the application of TJR implants, different surfaces have corresponding functional requirements, that is, osseointegrated surfaces require excellent biocompatibility owing to adhesion with bone cells, and articular surfaces require better biotribological performance owing to relative motion. To further improve the performance, a better approach is to differentiate osseointegrated surfaces and articular surfaces, particularly to attain higher biocompatibility of the osseointegrated surfaces and better biotribological properties of the articular surfaces.

In this study, we developed a novel one-step method through ion beam irradiation of DLC coatings by nitrogen ions to fabricate micropatterns for improving the biotribological properties of articular surfaces, and ion-irradiation-modified surfaces to improve the biocompatibility of osseointegrated surfaces. Furthermore, the relationships among irradiation conditions, mechanical properties, surface chemistry, and biocompatibility of the coatings were systematically assessed.

2 Experimental

2.1 Specimen preparation

Initially, the Ti6Al4V (Grade 5) substrates were cleaned in acetone, ethanol, and deionized water for 15 min in each medium. A DLC coating with a thickness of 200 nm and a titanium adhesion layer with a thickness of 100 nm were deposited onto a Ti6Al4V substrate with an area of 20 mm × 20 mm via magnetron sputtering under an argon atmosphere. Before the deposition process, the substrates were cleaned by RF plasma discharge at 50 W for 15 min. The initial pressure was 1×10^{-6} Torr. Graphite (99.99%) and titanium (99.99%) targets with a diameter of 100 mm were used, and both targets were pre-sputtered to eliminate contamination on the target surface. Subsequently, the DLC was deposited through a DC power source with a 40 Hz frequency, and the titanium sublayer was deposited with RF power of 150 W. The deposition pressure was maintained at 4.5×10^{-3} Torr. The coating thickness of each layer was controlled by the exposure time. The deposition rates of the DLC and titanium layers were 0.20 and 0.12 nm/s, respectively. To optimize the mechanical properties, a negative bias voltage was applied to the substrate at a voltage of –80 to 0 V.

2.2 Ion beam irradiation

The irradiation on the DLC coating was conducted using a customized ion beam system, and the nitrogen ion beam was generated using a commercial ion gun (PerkinElmer 04-303). The system was designed as a

dual vacuum circuit acting on a vacuum chamber and an ion gun. The chamber was evacuated to an initial pressure lower than 1×10^{-8} Torr. Irradiation was conducted under a vacuum pressure of 1×10^{-6} Torr. N_2 (99.9999%) was used as the gas source. To ensure uniform irradiation, the DLC-coated specimen was mounted on a motorized *XY* scan stage that was perpendicular to the ion beam. The scan speed was set to 0.2 mm/s and irradiation was performed on an area of 30 mm × 30 mm. The ion beam was defocused to a spot with a diameter of ~3 mm. The ion current was set to 1.5 μA, and the acceleration energy was 1 keV. The DLC coatings were modified under an irradiation dose of 2×10^{15}, 4×10^{15}, and 8×10^{15} ions/cm^2. Micropatterns were fabricated by masking the DLC coating with a commercial metal mesh, as shown in Fig. 1(a), to enhance the biotribological properties.

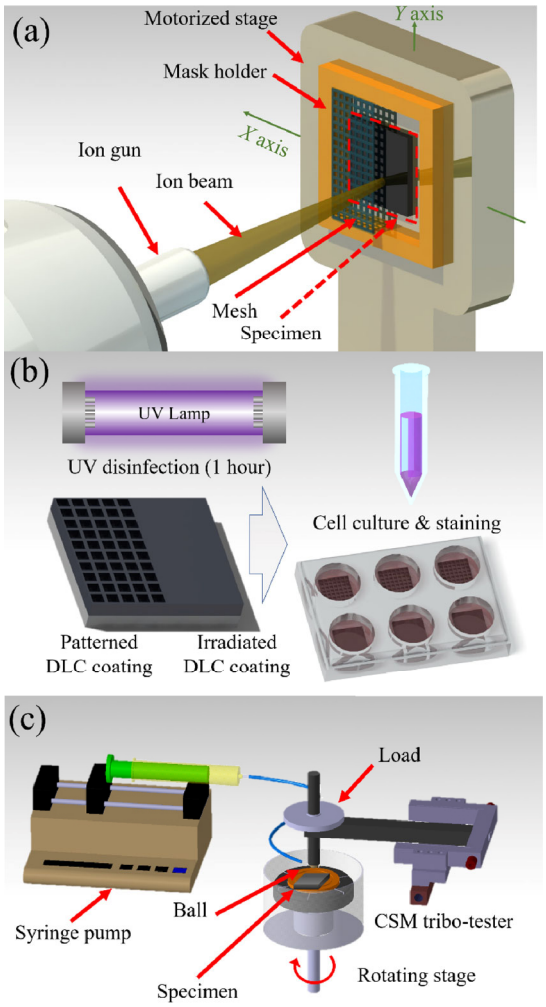

Fig. 1 Schematic illustrations of (a) the ion beam irradiation process, (b) cell culture and staining process, and (c) slid friction test.

A mesh with an aperture of 50 μm and a wire diameter of 30 μm was mounted on the DLC coating surface using a homemade holder. Half of the DLC coating was irradiated by the ion beam with the mask, forming the micropattern, while the rest was not covered by the mask.

2.3 Coating characterization

The hardness and modulus of the DLC coatings with different negative biases were evaluated using a high-precision ultra-nano hardness tester (UNHT, Anton Paar). The UNHT was employed with a round-ended Berkovich pyramid tip with a diameter of 20 μm. The surface roughness of the as-coated DLC and ion-beam-irradiated DLC coatings was characterized through atomic force microscopy (AFM, Park NX10). The dimensions and topographies of the patterned DLC coatings were measured by scanning electron microscopy (SEM, Jeol 6210) and a 3D laser scanning microscope (Keyence VK-X200K). The surface chemistry of the ion-beam-irradiated DLC coating was analyzed through *X*-ray photoelectron spectroscopy (XPS, Thermo Scientific, K-alpha).

2.4 Biocompatibility evaluation

The biocompatibility was evaluated by culturing MC3T3 cells on ion-beam-irradiated and micropatterned DLC coatings. A schematic of the cell culture and staining process is shown in Fig. 1(b). MC3T3-L1, a murine pre-osteoblastic cell line, was purchased from the American Type Culture Collection (Manassas, VA, USA). Cells were cultured at 37 °C in a humidified incubator under 5% CO_2 in α-MEM supplemented with 10% fetal bovine serum, 100 mg/mL streptomycin, and 100 U/mL penicillin. MC3T3-L1 cells were seeded at a density of 2×10^4 cells/cm^2 in a 6-well culture plate with ion-beam-irradiated and micropatterned DLC coatings. The specimens were sterilized by soaking in 70% ethanol overnight and by violet exposure for 2 h previously set on the well. After incubation for 24 h, the cells on the scaffolds were washed three times with phosphate-buffered saline (PBS) and fixed with 4% paraformaldehyde for 10 min. Eosin solution (1 ml eosin) was added to each well, and the cells were washed three times with PBS for cytoplasmic morphology staining for microscope observation.

2.5 Biotribological performance evaluation

A pin-on-disk type tribotester (CSM, TRB) was used to evaluate the biotribological behavior under wet sliding conditions lubricated by Ringer's solution [27]. The chemical makeup of Ringer's solution, which is typically used as the simulated body fluids for *in vitro* experiments, was 9.0 g/L NaCl, 0.48 g/L $CaCl_2$, 0.2 g/L $NaHCO_3$, and 0.42 g/L KCl [28]. To continuously supply Ringer's solution to the specimen surface, a syringe pump was employed with a flow rate of 1–3 mL/min depending on the rotation speed, as shown in Fig. 1(c). A stainless-steel ball with a 6 mm diameter was used as the stationary pin in the tribotests. The ball was slid against the specimen at rotation speeds of 50, 100, and 300 rpm, which were equivalent to 0.86, 1.73, and 5.18 m/min linear speed, respectively. Normal loads of 1, 2, and 5 N corresponding to the maximum Hertzian contact pressures of 523, 660, and 895 MPa, respectively, were applied. Tribotests were conducted at least three times to ensure repeatability and accuracy.

3 Results and discussion

3.1 Optimization of the DLC coating via bias voltage

According to previous research, the negative bias had a significant impact on the mechanical properties of the DLC coating and further affected the wear rate [29]. To optimize the mechanical properties of DLC coatings, the effect of negative bias voltage on the hardness was investigated, as shown in Fig. 2. The detailed nanoindentation behavior of the DLC coating under a maximum normal load of 0.15 mN is shown in Fig. 2(a). For all the specimens, the penetration depth was maintained at one-tenth of the total coating thickness to minimize the influence of the substrate. The coating deposited at 60 V had the lowest penetration depth of ~17 nm. It was found that delamination occurred when the DLC coating was deposited with a negative bias above –80 V, which was induced by high residual stress [8].

The hardness and modulus were calculated using the method of Oliver and Pharr [30], and the results are shown in Fig. 2(b). The hardness of the coating deposited at –60~0 V increased with the negative bias voltage, while the hardness of the coating deposited at –80 V was lower than that at –60 V. The highest hardness (23.4 GPa) was observed under a –60 V bias voltage. The Young's modulus revealed a similar tendency with the coating hardness. It is well documented that the hardness of DLC coating has a distinct critical value (60 V in this case) as the negative bias voltage increases [31, 32]. Initially, the ion energy increased as the negative bias voltage was applied to the substrate, and more sp^3 bonded carbon was deposited. Therefore, the hardness of the DLC coating increased. Conversely, when the negative bias voltage was greater than the critical value, it resulted in the deposition of sp^2 bonded carbon, which lowered the hardness of the DLC coating. Therefore, the DLC coatings in the subsequent research were all deposited under a bias voltage of –60 V.

3.2 Topography characterization

Figure 3 shows the AFM topography of as-coated DLC and DLC coating under irradiation doses of 2×10^{15}, 4×10^{15}, and 8×10^{15} ions/cm^2, and the corresponding average roughness value (R_a) of 11.68 ± 0.22, 2.25 ± 0.36, 2.23 ± 0.25, and 1.38 ± 0.14 nm, respectively. The

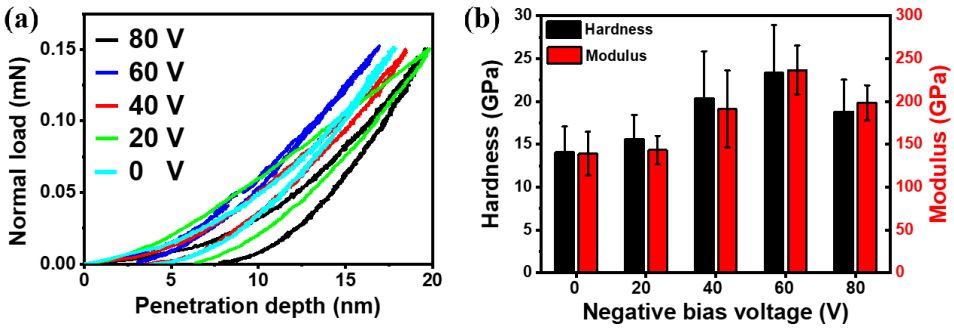

Fig. 2 (a) Nanoindentation load displacement and (b) hardness and modulus for the DLC coatings under negative bias voltage of 0, –20, –40, –60, and –80 V, respectively.

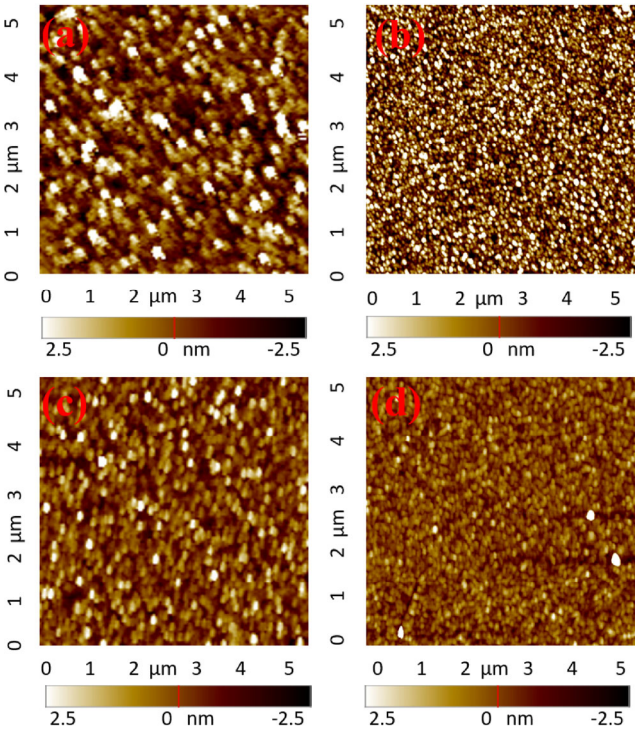

Fig. 3 Surface topographies of (a) as-coated DLC, and DLC coating after irradiation by N ions under irradiation does of (b) 2×10^{15}, (c) 4×10^{15}, and (d) 8×10^{15} ions/cm^2.

change in roughness was due to the increase of ion beam irradiation dose which caused the surface to be further polished. The polishing effect of the ion beam irradiation relies on material removal from the topmost surface via the kinetic interaction of energetic ions on the atoms or molecules of the surface [33].

For the masked specimens, micropatterns were fabricated after ion beam irradiation, and the pattern dimensions were evaluated using an SEM, as shown in Fig. 4(a). The depth of the pattern with different

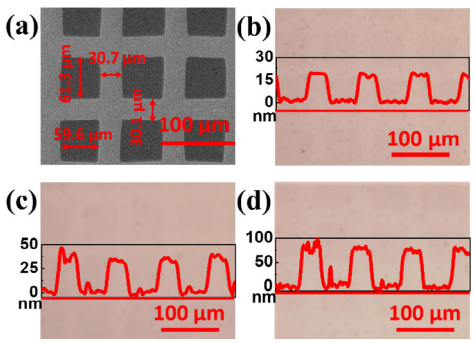

Fig. 4 (a) SEM images of micropatterned DLC coating; the optical image and 2D profile of micropatterned DLC coating under irradiation doses of (b) 2×10^{15}, (c) 4×10^{15}, and (d) 8×10^{15} ions/cm^2, respectively.

irradiation doses was verified by 3D confocal laser microscopy, and the results are shown in Figs. 4(b)–4(d). The pattern width was not significantly affected by the radiation dose. The depth of the pattern was ~19, ~37, and ~76 nm, which corresponded to radiation doses of 2×10^{15}, 4×10^{15}, and 8×10^{15} ions/cm^2, respectively. The pattern depth was linearly dependent on the ion dose under identical ion currents and acceleration energies.

3.3 Surface chemistry characterization

To further characterize the chemical composition of the ion-beam-irradiated DLC coatings, XPS analysis was conducted as shown in Fig. 5. The nitrogen concentration (at%) of the DLC irradiated under ion doses of 2×10^{15}, 4×10^{15}, and 8×10^{15} ions/cm^2 were 12.84%, 14.33%, and 15.46%, respectively. Owing to the upper limit of the nitrogen content in carbon materials, the concentration of nitrogen in the DLC tended to saturate as the irradiation dose increased [34]. Therefore, the nitrogen concentration of the irradiated specimens did not change significantly. Figures 5(a)–5(c) show the C 1s spectra of the ion-beam-irradiated DLC coating fitted by using a Gaussian-Lorentzian peak after Shirley background correction. Three carbon species, sp^2 C–C/sp^3 C–C (284.2 eV), sp^2 C–N (285.1 eV), and sp^3 C–N (287.0 eV) were deconvoluted [35, 36]. The N 1s peaks, as shown in Figs. 5(d)–5(f), were deconvoluted into 3 chemical bonds of N–O, sp^2 C–N, and sp^3 C–N at binding energy of 402.0, 399.6, and 398.0 eV, respectively [37]. It was apparent that as the irradiation dose increased, not only did the concentration of nitrogen in the DLC coating slightly increased but also the ratio of sp^3 C–N bonds. As a result, the unsaturated nitrogen bonds increased.

3.4 Ion beam irradiation and cell adhesion

The biocompatibility of ion-beam-irradiated DLC coatings was evaluated by the MC3T3 osteoblast adhesion test, as shown in Fig. 6. The cell coverage of both the ion beam patterned (Figs. 6(a)–6(c)) and irradiated (Figs. 6(d)–6(f)) DLC coating was improved significantly compared with the as-coated DLC (Fig. 6(g)). The comparison results of the cell coverage of MC3T3 cells as a function of irradiation dose for as-coated, irradiated, and patterned DLC coatings are

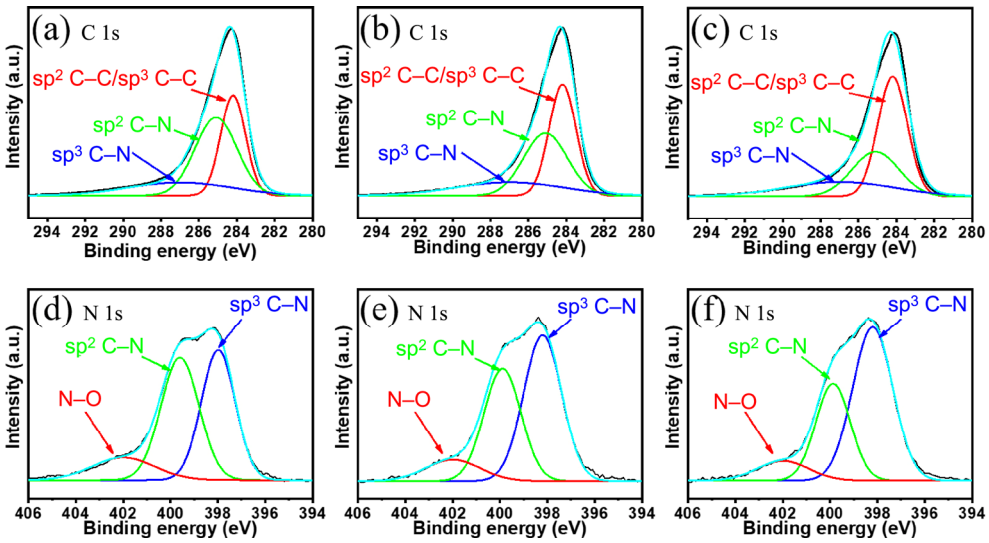

Fig. 5 XPS spectra C 1s of DLC coating under irradiation does of (a) 2×10^{15}, (b) 4×10^{15}, and (c) 8×10^{15} ions/cm^2. XPS spectra N 1s of DLC coating under irradiation doses of (d) 2×10^{15}, (e) 4×10^{15}, and (f) 8×10^{15} ions/cm^2.

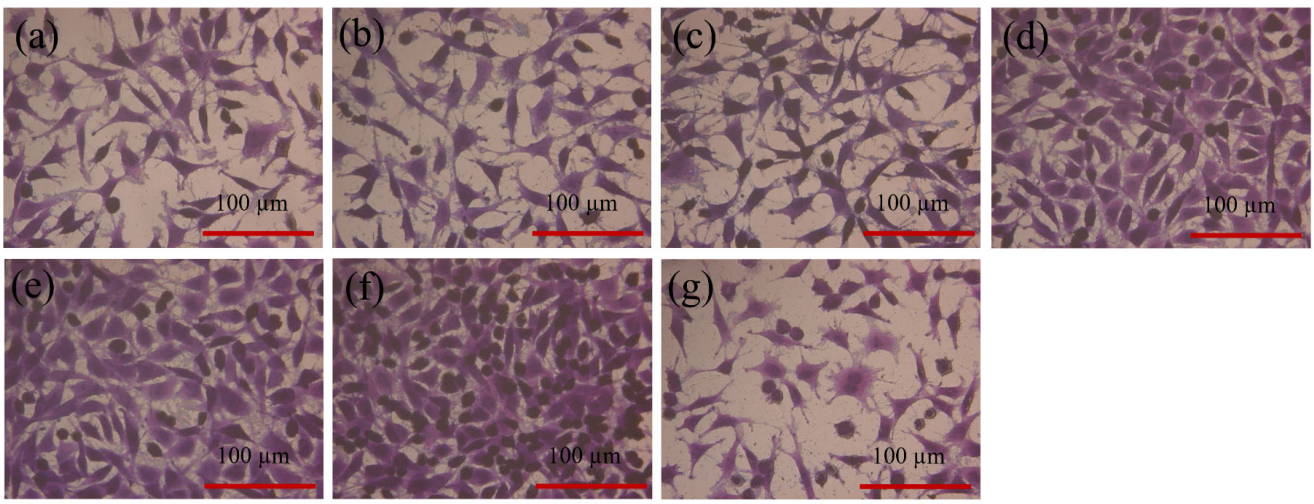

Fig. 6 Optical images of the MC3T3 cells on the ion beam patterned DLC under ion doses of (a) 2×10^{15}, (b) 4×10^{15}, and (c) 8×10^{15} ions/cm^2. Optical images of the MC3T3 cells on the ion-beam irradiated DLC under ion doses of (d) 2×10^{15}, (e) 4×10^{15}, (f) 8×10^{15} ions/cm^2, and (g) as-coated DLC.

shown in Fig. 7. With the increase in radiation dose, the cell coverage on both the series of patterned DLC and irradiated DLC increased. However, the overall coverage of the irradiated DLC was much higher than that of the patterned DLC with the same irradiation dose. Compared with the as-coated DLC, the cell coverage of irradiated DLC with an irradiation dose of 8×10^{15} ions/cm^2 increased from 32% to 86%. The optical images shown in Figs. 6(d)–6(f) demonstrate the morphology of the osteoblasts fixed on the surface of the ion-beam-irradiated DLC coatings. After one day of incubation, typical triangular cells attached to the

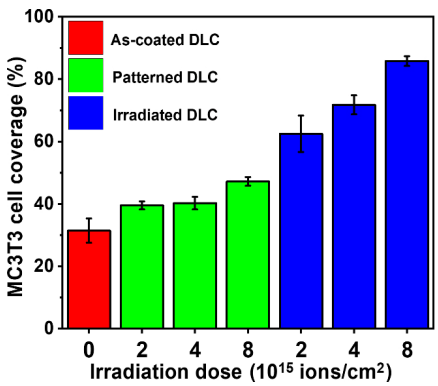

Fig. 7 Cell coverage for as-coated DLC, patterned DLC, and irradiated DLC as a function of irradiation dose.

surfaces of all specimens could be observed. It was found that nitrogen ion beam irradiation was significant for biocompatibility, and the cell adhesion coverage was promoted with an increase in the sp^3 C–N bond ratio. The results indicated that cell adhesion and growth on the irradiated DLC coatings were enhanced by non-specific binding between the nitrogen-enriched layer on the DLC surface and cell surface proteins.

For the patterned DLC coatings, cell adhesion depended not only on the surface chemical state but also on the surface morphology [38]. In the process of local adhesion establishment and maturation of the cells, topographical factors may act as direct physical interference. The micro-scale patterning elements were arranged in a symmetrical and regular manner, which can physically hinder the process of expansion and extension [39]. Some cells coated with specific extracellular proteins were even capable of detecting the geometric elements of the patterning size [40]. Moreover, the surface chemistry plays a more important role in this situation, and the ion beam irradiation on the micropatterned DLC performed only in the grooves. As a result, a low cell coverage on the micropatterned DLC was observed compared to the irradiated DLC, where the entire surface was irradiated with a nitrogen ion beam.

The frictional characteristics of the as-coated DLC and patterned DLC under the lubrication of Ringer's solution are shown in Fig. 8. The representative coefficient of friction (COF) curves of the as-coated DLC and patterned DLC with respect to the sliding cycle under a normal load of 1 N and 100 rpm are shown in Fig. 8(a). The COF of the patterned DLC fabricated under an irradiation dose of 4×10^{15} ions/cm^2 with respect to the rpm is shown in Fig. 8(b). The tribotests performed to assess the effects of speed were carried out under a normal load of 1 N, and the results are summarized in Fig. 8(c). At a low rotation speed of 50 rpm, the COF of all the specimens tended to be the same. At relatively high speeds of 100 and 300 rpm, the micropatterned DLC coatings showed better lubricating properties than the as-coated DLC coatings. This was because the surface patterns functioned as micro-hydrodynamic bearings which increased the fluid pressure, thereby increasing the overall load-carrying capacity [26]. This effect became more apparent as the speed increased, and the COF was significantly reduced at 100 and 300 rpm. The micropattern with a depth

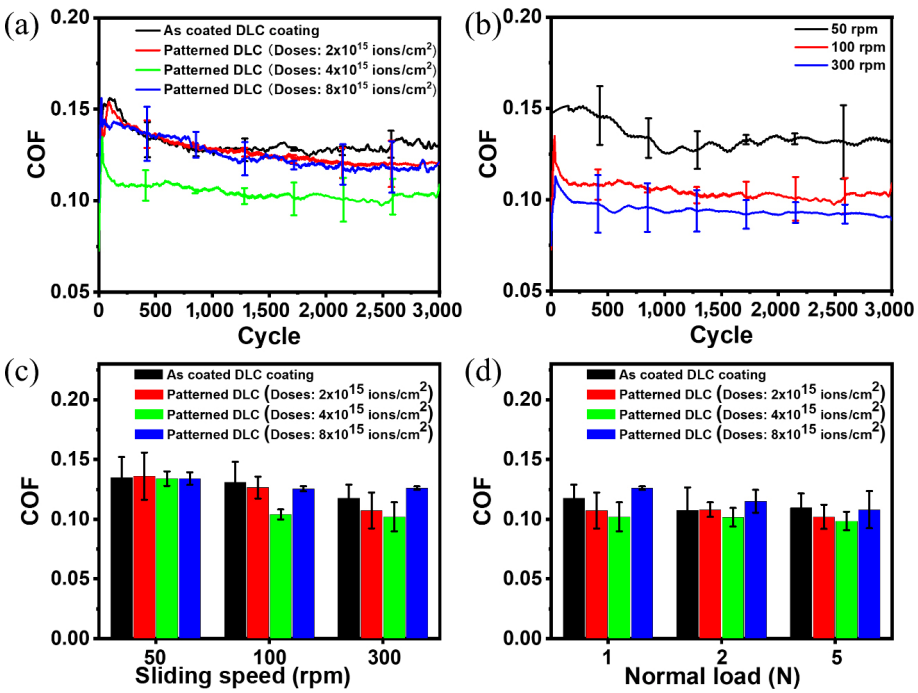

Fig. 8 COF with respect to (a) sliding cycle for the as-coated DLC and patterned DLC under the normal load of 1 N and 100 rpm. (b) The sliding cycle for the patterned DLC under ion dose of 4×10^{15} ions/cm^2. Further, the biotribological behavior of the as-coated DLC and patterned DLC with respect to (c) sliding speed and (d) normal load.

of 37 nm exhibited good friction properties, and the COF was reduced by 21% at relatively high speeds. Conversely, the friction behavior of the patterned coating fabricated by ion doses of 8×10^{15} ions/cm^2 was similar or inferior to that of the as-coated DLC, which was due to its relatively steep geometric pattern. Steep patterns led to undesired edge effects, thus increasing the COF and counterbalancing the beneficial effects induced by the surface patterning [41]. Moreover, the residual stress of the coating due to surface patterning may influence the mechanical properties of the DLC coatings, especially the fatigue properties [42]. As the depth of the fabricated pattern increased, the residual stress on the surface increased accordingly [43]. The consequent negative effect was that the patterning layer was more likely to succumb to abrasion and cause an increase in the friction. The tribotests on the normal load were performed at a rotation speed of 300 rpm, as shown in Fig. 8(d). The influence of normal load on the COF was insignificant, and the overall trend was that as the normal load increased, the COF decreased slightly. Comparing the patterned DLC coating under different irradiation doses, the trend of the COF with respect to the normal load was similar to that of the sliding speed.

Figure 9 shows the lubrication mechanism of the as-coated DLC and ion beam patterned DLC lubricated by Ringer's solution. Compared to the as-coated DLC, the COF of the patterned DLC under an ion dose of 2×10^{15} ions/cm^2 was not significantly reduced. It can be assumed that the depth of the patterned DLC under an ion dose of 2×10^{15} ions/cm^2 was not sufficient to store the wear particles and provide hydrodynamic effects, as shown in Figs. 9(a) and 9(b), respectively. In both cases, the wear particles remained in the middle of the wear track inducing further wear and ultimately led to a higher COF. For the patterned DLC under an ion dose of 4×10^{15} ions/cm^2, the COF had a relatively significant reduction, which could be explained by the pattern providing effective additional load-carrying capacity and wear particle trapping, as shown in Fig. 9(c). Though the patterned DLC under an ion dose of 8×10^{15} ions/cm^2 also possessed a similar function, the steep pattern led to edge effects that increased the COF, as shown in Fig. 9(d). In addition, the surface residual stress also increased with the increase in pattern depth, which may induce the pattern to succumb to wear and cause higher friction. Patterned DLC can effectively avoid three-body abrasive wear and corrosive wear benefitted from the wear debris trapping effect of micropattern and the inertness of DLC to the body fluid environment [5, 44]. Therefore, the wear behaviors of patterned DLC coating were mainly dominated by two-body abrasive wear and adhesive wear [45, 46].

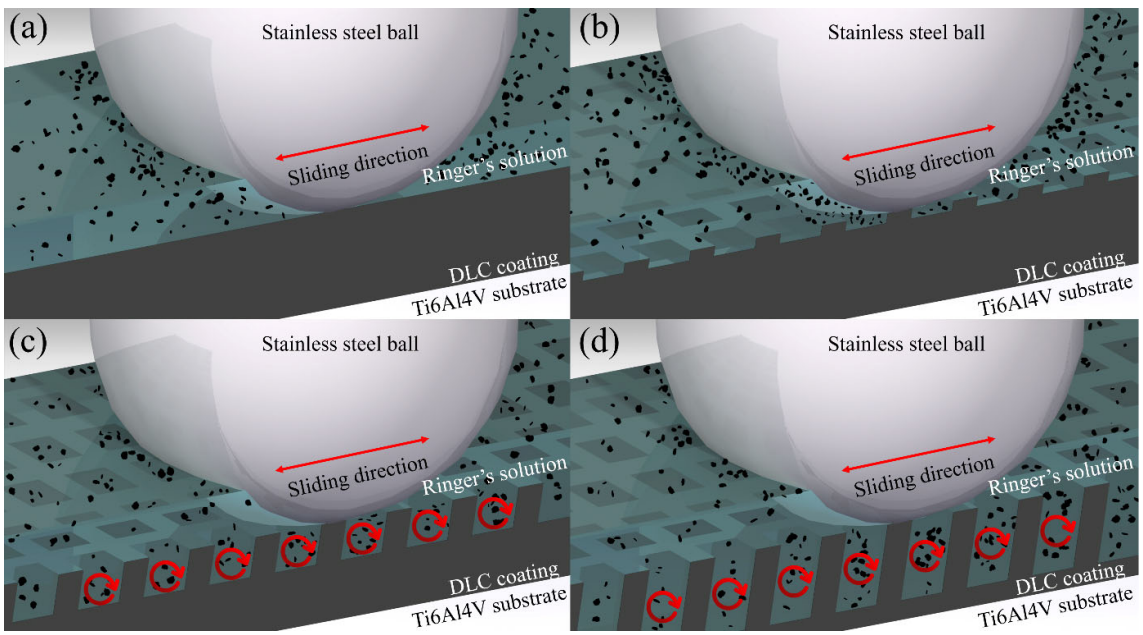

Fig. 9 Schematic illustration of the lubrication mechanism of (a) as-coated DLC coating; ion beam patterned DLC under ion doses of (b) 2×10^{15}, (c) 4×10^{15}, and (d) 8×10^{15} ions/cm^2.

Previous studies have documented the influence of a negative bias on the structure and performance of the DLC prepared by magnetron sputtering [8, 22]. The increase in the negative bias voltage may increase the ion energy, which aided in reducing the graphite clusters with weaker carbon atoms, thereby increasing the sp^3 fraction. The content of sp^3 structure did not necessarily increase with the increase in ion energy, which provided the maximum sp^3 fraction at certain values of bias voltage (–60 V in this case), as proven in this study. When the bias voltage increased further, higher energy ions caused the sp^3 bond to break, resulting in a decrease in hardness. Altering the DLC coating with increased hardness by applying a negative voltage proved to be an effective means to improve its friction reduction performance. Consequently, the DLC coating optimized under –60 V was considered as a desirable candidate for further modification via patterning and irradiation with the nitrogen ion beam [29].

The surface chemical state of TJR implants determines their interaction with surrounding cells and tissues and plays a decisive role in the success of the implant. The ability of the coated surface to promote cell adhesion depends on the extent to which they adsorb proteins in a medium that interacts with cell surface receptors [47]. Therefore, the interaction between the functional groups on the coating surface and the protein is the key factor influencing cell adhesion. In a study of protein functional groups and cell electrical properties, it was pointed out that protein distal ends of osteoblast cells have SH, PO_3, NH_2, and COOH groups [48]. Among them, the SH groups typically have a neutral charge and NH_2 groups tend to be positively charged, while the PO_3 and COOH groups are negatively charged. Therefore, an ordered surface with functional groups can serve as a site for cell growth. The nitrogen ion beam irradiation induced functional sp^2 C–N and sp^3 C–N bonds on the topmost surface of the DLC coatings, which resulted in the polarization on the DLC surface owing to the difference in electronegativity between carbon and nitrogen [49]. Moreover, as the radiation dose increased, the nitrogen content of the DLC coating increased. In addition, the proportion of sp^2 C–N bonds decreased, whereas the proportion of sp^3 C–N bonds increased (Fig. 5), and the unsaturation of N bonds increased. Therefore, the number of proteins attached to the surface of the material increased with an increase in the degree of unsaturated N bonds, which promoted the biocompatibility of the irradiated DLC coatings.

The surface chemistry and morphology of DLC were modified by a low-energy ion beam, which benefited from its physical properties by sputtering the energetic ions to interact with the coating surface. Although the low-energy ion beam is a vacuum process, it has some shortcomings, such as difficulty in the *in-situ* control of the pattern depth. However, it has advantages such as, no contact, no load, no edge effects, and high efficiency. In this study, the two effects of low-energy ion beams, surface chemical modification and topographic material removal, have been effectively applied in the application of DLC-coated surfaces for TJR implants. Surface chemical modification adjusted the ratio of unsaturated N bonds and enhanced the cell adhesion of the irradiated DLC coating. Moreover, because the penetration depth was less than 10 nm, irradiation did not significantly affect the mechanical properties of the DLC. Regarding the biotribological performance of the micropatterned DLC, it was found that a pattern that was too deep could increase the COF owing to residual stress (Fig. 9(d)). This outcome may be overcome by further optimization of the micropattern geometry.

4 Conclusions

A one-step surface modification method for DLC coating through low energy irradiation of a nitrogen ion beam was proposed to enhance the biocompatibility of osseointegrated surfaces and biotribological performance of articular surfaces. Superior mechanical properties were achieved by optimizing the bias voltage. The adhesion of MC3T3 osteoblasts increased significantly from 32% to 86% under an irradiation dose of 8×10^{15} ions/cm^2. In addition, nitrogen ion beam irradiation was proven to be an effective method to increase cell adhesion due to the enhanced interaction of unsaturated sp^3 C–N bonds on the DLC surface with surface functional groups of osteoblast proteins. Furthermore, ion beam micropatterning enhanced the frictional performance of the DLC in simulated body fluid lubrication environment. Thus, the DLC coating irradiated by nitrogen ion beam using the proposed one-step method has great potential applicability in the orthopedic implant industry.

Acknowledgements

This study was supported by National Research Foundation of Korea (NRF) grant funded by the Korean government (MSIT) (No. 2020R1A2C2004714) and funding from the State Key Laboratory of Solidification Processing in NWPU (No. SKLSP202002).

References

[1] Etkin C D, Springer B D. The American joint replacement registry-the first 5 years. *Arthroplast Today* **3**(2): 67–69 (2017)

[2] Delanois R E, Mistry J B, Gwam C U, Mohamed N S, Choksi U S, Mont M A. Current epidemiology of revision total knee arthroplasty in the United States. *J Arthroplasty* **32**(9): 2663–2668 (2017)

[3] Kang Y K, Kim M H, Kim J W, Tien T, Lim D H, Chun H J. Analysis on wear phenomenon of artificial knee joint based on FEM and mechanical test. *Int J Precis Eng Man* **19**(8): 1211–1217 (2018)

[4] Groll J, Fiedler J, Bruellhoff K, Moeller M, Brenner R E. Novel surface coatings modulating eukaryotic cell adhesion and preventing implant infection. *Int J Artif Organs* **32**(9): 655–662 (2009)

[5] Lee H H, Lee S, Park J K, Yang M. Friction and wear characteristics of surface-modified titanium alloy for metal-on-metal hip joint bearing. *Int J Precis Eng Man* **19**(6): 917–924 (2018)

[6] Agarwal S. Osteolysis - basic science, incidence and diagnosis. *Curr Orthopaed* **18**(3): 220–231 (2004)

[7] Penkov O V, Pukha V E, Starikova S L, Khadem M, Starikov V V, Maleev M V, Kim D E. Highly wear-resistant and biocompatible carbon nanocomposite coatings for dental implants. *Biomaterials* **102**: 130–136 (2016)

[8] Penkov O V, Khadem M, Lee J S, Kheradmandfard M, Kim C L, Cho S W, Kim D E. Highly durable and biocompatible periodical Si/DLC nanocomposite coatings. *Nanoscale* **10**(10): 4852–4860 (2018)

[9] Hauert R. A review of modified DLC coatings for biological applications. *Diam Relat Mater* **12**(3–7): 583–589 (2003)

[10] Giorleo L, Montesano L, La Vecchia G M. Laser surface texturing to realize micro-grids on DLC coating: effect of marking speed, power, and loop cycle. *Int J Precis Eng Man* **22**(5): 745–758 (2021)

[11] Dearnaley G, Arps J H. Biomedical applications of diamond-like carbon (DLC) coatings: A review. *Surf Coat Tech* **200**(7): 2518–2524 (2005)

[12] Randeniya L, Bendavid A, Martin P, Cairney J, Sullivan A, Webster S, Proust G, Tang F, Rohanizadeh R. Thin film composites of nanocrystalline ZrO(2) and diamond-like carbon: Synthesis, structural properties and bone cell proliferation. *Acta Biomater* **6**(10): 4154–4160 (2010)

[13] Hauert R, Falub C V, Thorwarth G, Thorwarth K, Affolter C, Stiefel M, Podleska L E, Taeger G. Retrospective lifetime estimation of failed and explanted diamond-like carbon coated hip joint balls. *Acta Biomaterialia* **8**(8): 3170–3176 (2012)

[14] Hasebe T, Yohena S, Kamijo A, Okazaki Y, Hotta A, Takahashi K, Suzuki T. Fluorine doping into diamond-like carbon coatings inhibits protein adsorption and platelet activation. *J Biomed Mater Res A* **83**(4): 1192–1199 (2007)

[15] Shao W, Zhao Q, Abel E W, Bendavid A. Influence of interaction energy between Si-doped diamond-like carbon films and bacteria on bacterial adhesion under flow conditions. *J Biomed Mater Res A* **93**(1): 133–139 (2010)

[16] Filova E, Vandrovcova M, Jelinek M, Zemek J, Houdkova J, Jan R, Kocourek T, Stankova L, Bacakova L. Adhesion and differentiation of Saos-2 osteoblast-like cells on chromium-doped diamond-like carbon coatings. *J Mater Sci Mater Med* **28**(1): 17 (2017)

[17] Zhang M, Xie T, Qian X, Zhu Y, Liu X. Mechanical properties and biocompatibility of Ti-doped diamond-like carbon films. *ACS Omega* **5**(36): 22772–22777 (2020)

[18] Bociaga D, Komorowski P, Batory D, Szymanski W, Olejnik A, Jastrzebski K, Jakubowski W. Silver-doped nanocomposite carbon coatings (Ag–DLC) for biomedical applications - Physiochemical and biological evaluation. *Appl Surf Sci* **355**: 388–397 (2015)

[19] Asri R I M, Harun W S W, Samykano M, Lah N A C, Ghani S A C, Tarlochan F, Raza M R. Corrosion and surface

modification on biocompatible metals: A review. *Sci Eng C Mater Biol Appl* **77**: 1261–1274 (2017)

[20] Allen M, Myer B, Rushton N. *In vitro* and *in vivo* investigations into the biocompatibility of diamond-like carbon (DLC) coatings for orthopedic applications. *J Biomed Mater Res* **58**(3): 319–328 (2001)

[21] Nakamura T, Ohana T. Photochemical modification of DLC films with oxygen functionalities and their chemical structure control. *Diam Relat Mater* **33**: 16–19 (2013)

[22] Penkov O V, Kheradmandfard M, Khadem M, Kharaziha M, Mirzaamiri R, Seo K J, Kim D E. Ion-beam irradiation of DLC-based nanocomposite: Creation of a highly biocompatible surface. *Appl Surf Sci* **469**: 896–903 (2019)

[23] Feng H Q, Wang G M, Wu G S, Jin W H, Wu H, Chu P K. Plasma and ion-beam modification of metallic biomaterials for improved anti-bacterial properties. *Surf Coat Tech* **306**: 140–146 (2016)

[24] Ziberi B, Frost F, Hoche T, Rauschenbach B. Ripple pattern formation on silicon surfaces by low-energy ion-beam erosion: Experiment and theory. *Phys Rev B* **72**(23): 235310 (2005)

[25] Hwang I T, Jung C H, Jung C H, Choi J H, Shin K, Yoo Y D. Simple and biocompatible ion beam micropatterning of a cell-repellent polymer on cell-adhesive surfaces to manipulate cell adhesion. *J Biomed Nanotechnol* **12**(2): 387–393 (2016)

[26] Allen Q, Raeymaekers B. Surface texturing of prosthetic hip implant bearing surfaces: A review. *J Tribol-T Asme* **143**(4): 040801 (2021)

[27] Kheradmandfard M, Kashani-Bozorg S F, Lee J S, Kim C-L, Hanzaki A Z, Pyun Y-S, Cho S-W, Amanov A, Kim D-E. Significant improvement in cell adhesion and wear resistance of biomedical β-type titanium alloy through ultrasonic nanocrystal surface modification. *J Alloy Compd* **762**: 941–949 (2018)

[28] Jin W H, Chu P K. Surface functionalization of biomaterials by plasma and ion beam. *Surf Coat Tech* **336**: 2–8 (2018)

[29] Khadem M, Park T L, Penkov O V, Kim D E. Highly transparent micro-patterned protective coatings on polyethylene terephthalate for flexible solar cell applications. *Sol Energy* **171**: 629–637 (2018)

[30] Oliver W C, Pharr G M. Measurement of hardness and elastic modulus by instrumented indentation: Advances in understanding and refinements to methodology. *J Mater Res* **19**(1): 3–20 (2004)

[31] Bugaev S P, Podkovyrov V G, Oskomov K V, Smaykina S V, Sochugov N S. Ion-assisted pulsed magnetron sputtering deposition of ta-C films. *Thin Solid Films* **389**(1–2): 16–26 (2001)

[32] Bernhardt F, Georgiadis K, Dolle L, Dambon O, Klocke F. Development of a ta-C diamond-like carbon (DLC) coating by magnetron sputtering for use in precision glass molding. *Materialwiss Werkst* **44**(8): 661–666 (2013)

[33] Savvides N. Surface microroughness of ion-beam etched optical surfaces. *J Appl Phys* **97**(5): 053517 (2005)

[34] Zhang S, Tsuzuki S, Ueno K, Dokko K, Watanabe M. Upper limit of nitrogen content in carbon materials. *Angew Chem Int Ed Engl* **54**(4): 1302–1306 (2015)

[35] Zhao M, Cao Y, Liu X, Deng J, Li D, Gu H. Effect of nitrogen atomic percentage on N^+-bombarded MWCNTs in cytocompatibility and hemocompatibility. *Nanoscale Res Lett* **9**(1): 142 (2014)

[36] Ayiania M, Smith M, Hensley A J R, Scudiero L, McEwen J S, Garcia-Perez M. Deconvoluting the XPS spectra for nitrogen-doped chars: An analysis from first principles. *Carbon* **162**: 528–544 (2020)

[37] Gao J, Wang Y, Wu H, Liu X, Wang L, Yu Q, Li A, Wang H, Song C, Gao Z, et al. Construction of a sp(3) /sp(2) carbon interface in 3D N-doped nanocarbons for the oxygen reduction reaction. *Angew Chem Int Ed Engl* **58**(42): 15089–15097 (2019)

[38] Al Qahtani W M, Schille C, Spintzyk S, Al Qahtani M S, Engel E, Geis-Gerstorfer J, Rupp F, Scheideler L. Effect of surface modification of zirconia on cell adhesion, metabolic activity and proliferation of human osteoblasts. *Biomed Eng Biomed Tech* **62**(1): 75–87 (2017)

[39] Robotti F, Bottan S, Fraschetti F, Mallone A, Pellegrini G, Lindenblatt N, Starck C, Falk V, Poulikakos D, Ferrari A. A micron-scale surface topography design reducing cell adhesion to implanted materials. *Sci Rep* **8**(1): 10887 (2018)

[40] Bottan S, Robotti F, Jayathissa P, Hegglin A, Bahamonde N, Heredia-Guerrero J A, Bayer I S, Scarpellini A, Merker H, Lindenblatt N, et al. Surface-structured bacterial cellulose with guided assembly-based biolithography (GAB). *ACS Nano* **9**(1): 206–219 (2015)

[41] Zhang J J, Zhang J G, Rosenkranz A, Zhao X L, Song Y L. Surface textures fabricated by laser surface texturing and diamond cutting-influence of texture depth on friction and wear. *Adv Eng Mater* **20**(4): 1700995 (2018)

[42] Srinivasan N, Bhaskar L K, Kumar R, Baragetti S. Residual stress gradient and relaxation upon fatigue deformation of diamond-like carbon coated aluminum alloy in air and methanol environments. *Mater Design* **160**: 303–312 (2018)

[43] Shen S G, Li B Z, Guo W C. Experimental study on grinding-induced residual stress in C–250 maraging steel. *Int J Adv Manuf Tech* **106**(3–4): 953–967 (2020)

[44] Choi H W, Lee K R, Park S J, Wang R, Kim J G, Oh K H.

Effects of plastic strain of diamond-like carbon coated stainless steel on the corrosion behavior in simulated body fluid environment. *Surf Coat Tech* **202**(12): 2632–2637 (2008)

[45] Hokkirigawa K, Kato K. An Experimental and Theoretical Investigation of Plowing, Cutting and Wedge Formation during Abrasive Wear. *Tribol Int* **21**(1): 51–57 (1988)

[46] Zhang J S, Yang H D, Chen S H, Tang H H. Study on the influence of micro-textures on wear mechanism of cemented carbide tools. *Int J Adv Manuf Tech* **108**(5–6): 1701–1712 (2020)

[47] Ferrari A C, Rodil S E, Robertson J. Interpretation of infrared and Raman spectra of amorphous carbon nitrides. *Phys Rev B* **67**(15): 155306 (2003)

[48] Tew L S, Ching J Y, Ngalim S H, Khung Y L. Driving mesenchymal stem cell differentiation from self-assembled monolayers. *Rsc Adv* **8**(12): 6551–6564 (2018)

[49] Takemoto S, Kusudo Y, Tsuru K, Hayakawa S, Osaka A, Takashima S. Selective protein adsorption and blood compatibility of hydroxy-carbonate apatites. *J Biomed Mater Res A* **69**(3): 544–551 (2004)

Yuzhen LIU. He is a Ph.D. student in Triblology Research Lab at Department of Mechanical Engineering of Yonsei University. Currently, he is focusing on *in-situ* micro-Raman spectroscopy analysis and microstructural impact on tribological behaviors. He previously pursued his master's degree in Chonbuk National University.

Kelun ZHANG. She received a master degree from Yonsei University in 2018. Then she turned to the Department of Medical Sciences to pursue a Ph.D. degree. Her research is designed into the field of biomedicine through *in vitro* and *in vivo* experiments, as well as the research on the function of human immune cells and the mechanism of immune response, especially in skin immunity.

Jae-Ho HAN. He received his B.S. degree in Department of Aeronautical and Mechanical Design Engineering from Korea National University of Transportatio in 2016. Currently, he is a Ph.D. student at Yonsei University. His research interests include acoustic emission generated by frictional behavior and tribological characteristics of micro-patterns.

Youn-Hoo HWANG. He received his B.S. and M.S. degrees in Department of Precision Mechanical Engineering from Kyungpook National University in 2019. Currently, he is a Ph.D. candidate at Yonsei University. His research interests include tribological characteristics of coating in various environments and wear reduction mechanisms.

Shusheng XU. He is currently a professor in State Key Laboratory of Solid Lubrication (LSL), Chinese Academy of Sciences, China. Before joining LSL, he worked as a research fellow in the University of Leeds from February 2018 to January 2020, and a postdoctoral research associate in Yonsei University from August 2016 to January 2018. The main research interest of his group is design and preparation of functional coating for surface engineering. His research interests include the vapor deposition of film materials for addressing the growth mechanism and film structure design, especially the transition metal dichalcogenides, ceramic, and DLC film materials, and their applications in extreme space environments. Currently, he have published more than 30 papers and gotten 5 patents for invention.

Dae-Eun KIM. He is a professor at the School of Mechanical Engineering at Yonsei University. Prof. Kim received his B.S. degree from Tufts University, and M.S. and Ph.D. degrees from Massachusetts Institute of Technology. He was an assistant professor at Ohio State University before joining Yonsei University in 1993. Prof. Kim served as the president of the Korean Tribology Society, president of the Korean Society for Precision Engineering, chair of the Tribology Technical Committee of International Federation for the Promotion of Mechanism and Machine Science (IFToMM), editor-in-chief of *International Journal of Precision Engineering and Manufacturing (IJPEM)*, senior editor of *Journal of Mechanical Science and Technology (JMST)*, and associate editor of *The American Society of Mechanical Engineers Journal (ASME J) of Tribology*. Prof. Kim is currently involved in the editorial boards of *Tribology Letters*, *Advances in Tribology*, *Friction*, *Frontiers in Mechanical Engineering*, *International Journal of Precision Engineering and Manufacturing-Green Technology (IJPEM-GT)*, *Lubricants*, and *Tribology Online*.